Supplementary Figures and Legends

Loss of the Tumor Suppressor Snf5 Leads to Aberrant Activation of the Hedgehog-Gli Pathway

Authors: Zainab Jagani, E. Lorena Mora-Blanco, Courtney G. Sansam, Elizabeth S. McKenna, Boris Wilson, Dongshu Chen, Justin Klekota, Pablo Tamayo, Phuong T.L. Nguyen, Michael Tolstorukov, Peter J. Park, Yoon-Jae Cho, Kathy Hsiao, Silvia Buonamici, Scott L. Pomeroy, Jill P. Mesirov, Heinz Ruffner, Tewis Bouwmeester, Sarah J. Luchansky, Joshua Murtie,Joseph F. Kelleher, Markus Warmuth, William R. Sellers, Charles W. M. Roberts, and Marion Dorsch

Nature Medicine: doi:10.1038/nm.2251

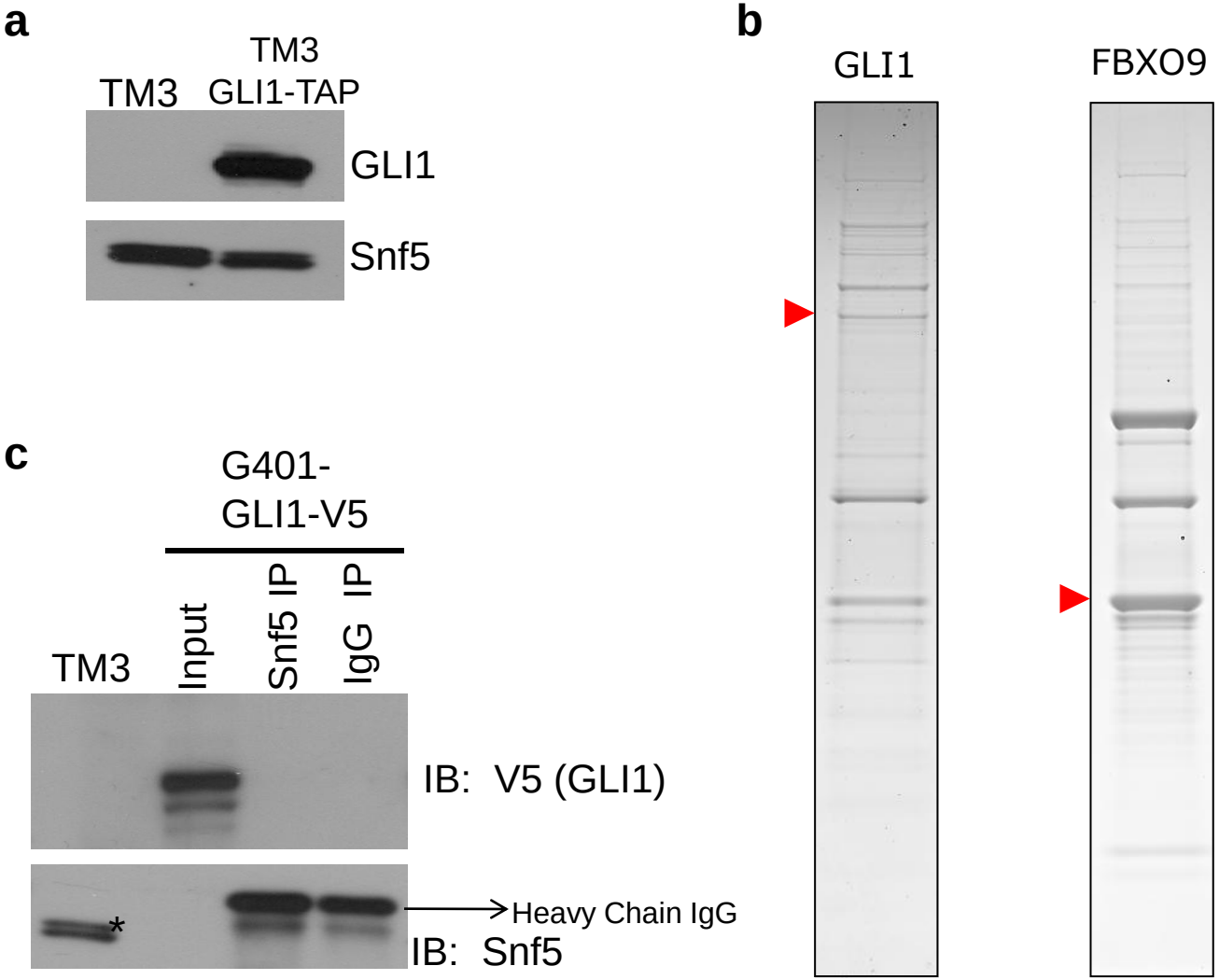

Nature Medicine: doi:10.1038/nm.2251

Supplementary Figure 1. Expression and Purification of TAP-tagged GLI1 Protein and failure of GLI1 to immunoprecipitate with a Snf5 antibody in SNF5-deficient G401 cells transiently expressing V5-GLI1. **(a)** Western blot indicating expression of TAP-tagged GLI1 in TM3 cells. While in theory, any IgG antibody should be able to detect a TAP-tagged protein due to the presence of an IgG binding domain, we used a GLI1 antibody in this immunoblot. The lysates were probed with Snf5 antibody as a control. **(b)** TAP-tagged GLI1 was purified using the standard two step TAP purification procedure and the purified protein complexes were separated using denaturing gel electrophoresis (SDS-PAGE). A Coomassie stained gel is shown indicating GLI1 (red arrow) and associated proteins on the left gel, and the right gel shows the purification of an unrelated protein FBXO9 (red arrow) and its associated proteins. **(c)** Whole cell lysates from SNF5-deficient G401 malignant rhabdoid tumor cells over-expressing V5-GLI1 were subjected to immunoprecipitation (IP) with a Snf5 antibody or a control IgG. Subsequent immunoblotting with a V5 antibody showed GLI1(V5) expression in input controls, but not in Snf5 IPs or IgG IPs, as G401 cells lack SNF5 expression show in the the blot below. TM3 whole cell lysate serves as a positive control for Snf5 expression (denoted with an *), and no SNF5 expresion is detected in G401 input, nor in G401 IPs. The heavy chain IgG is shown in the IPs (with a lighter background band that appears beneath, but that is distinct from the Snf5 doublet band that is shown in the TM3 cells positive control (first lane, lower blot)

Nature Medicine: doi:10.1038/nm.2251

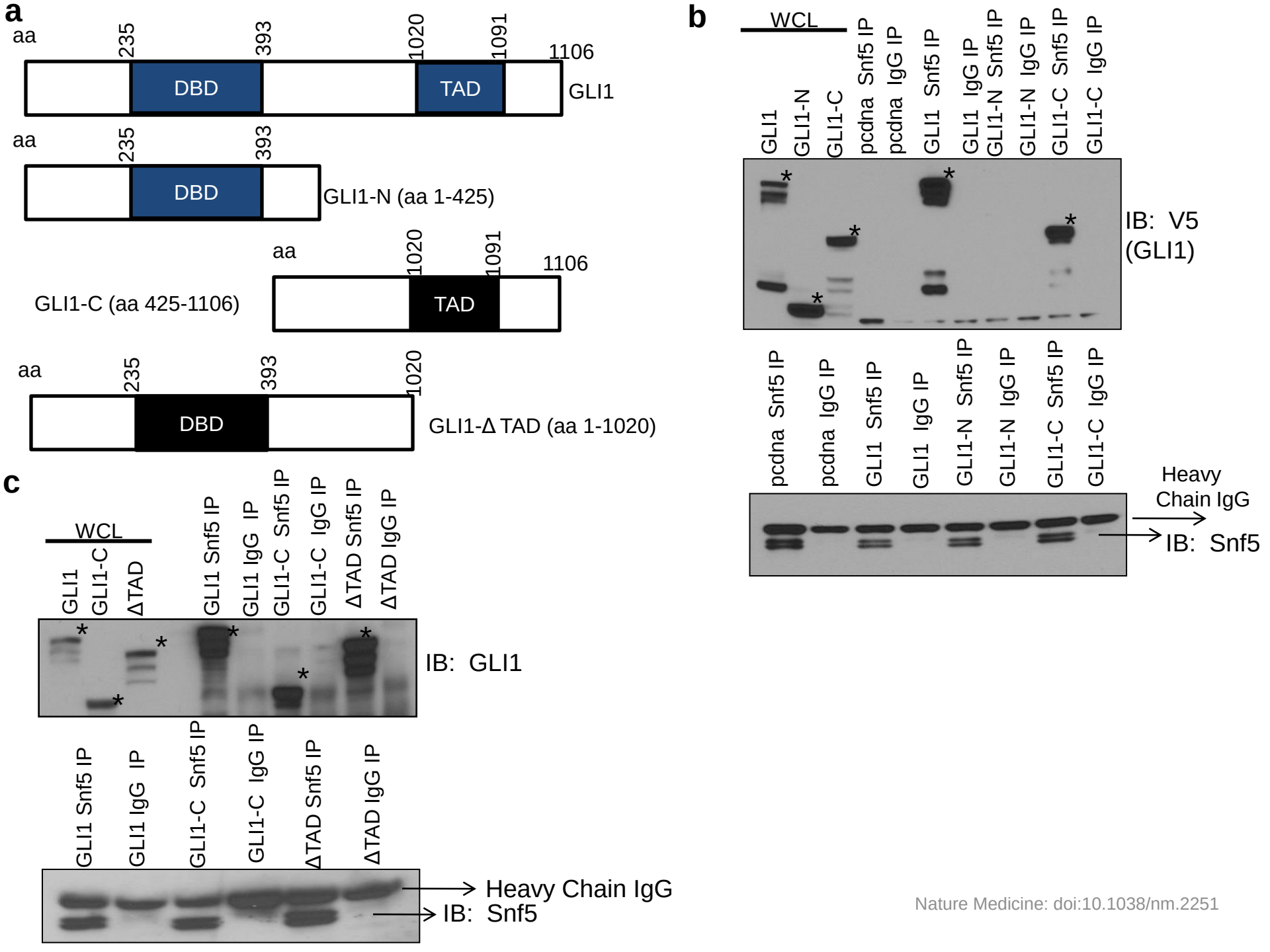

Nature Medicine: doi:10.1038/nm.2251

Supplementary Figure 2. Snf5 Interacts with the C-terminal Domain of GLI1. (a) Structure of GLI1 protein domains and the deletion constructs that were used to test interaction with Snf5. **(b)** Whole cell lysates from TM3 cells over-expressing V5 tagged WT GLI1, GLI1-N (1-425), or GLI-C (425-1106) were subjected to immunoprecipitation (IP) of endogenous Snf5 with a Snf5 antibody or a control IgG. Subsequent immunoblotting (IB) with a V5 antibody revealed co-immunoprecipitation of WT GLI1 and GLI1-C(425-1106) but not GLI-N (1-425). * denotes the expected size for the respective GLI1 proteins. A control blot indicating successful immunoprecipitation of Snf5 is shown below. **(c)** Experiments as in b, but comparing interaction of Snf5 with WT GLI1, GLI1-C (425-1106), or GLI1ΔTAD (1-1020). Snf5 interacts with both GLI1-C and and GLI1ΔTAD (1-1020).

Nature Medicine: doi:10.1038/nm.2251

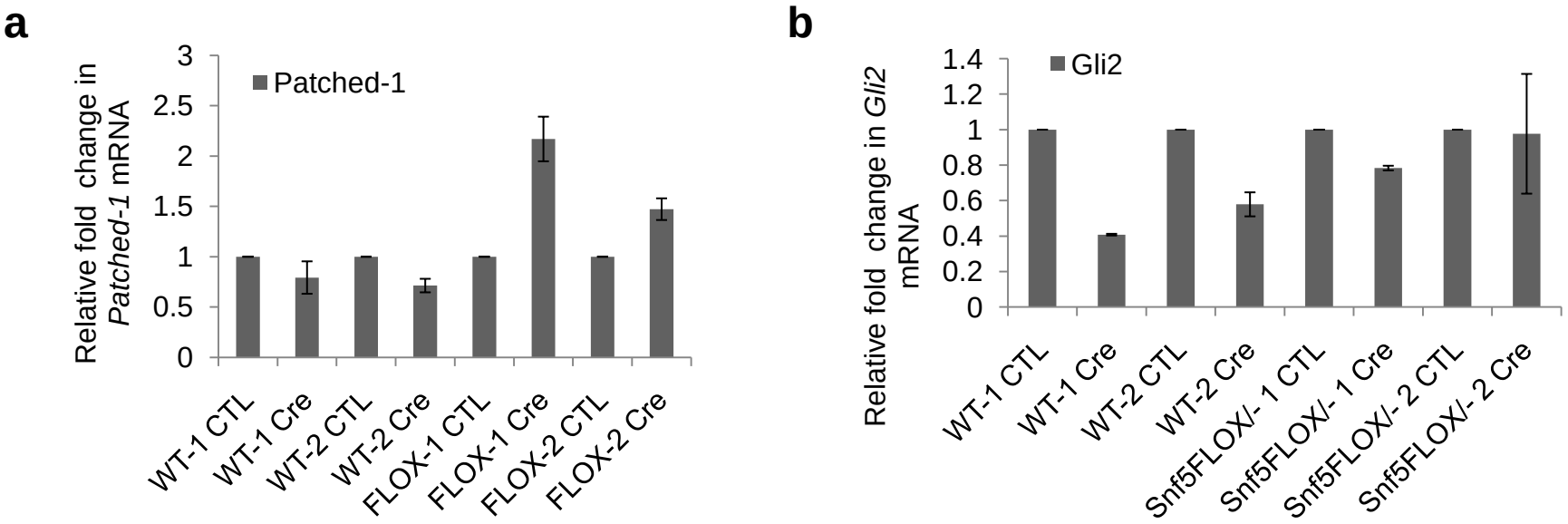

Supplementary Figure 3. Expression of Patched1 and Gli2 upon Snf5 loss in primary mouse embryonic fibroblasts (MEFs). (a) qRT-PCR showing an increase in *Patched-1* mRNA expression in Cre-treated Snf5FLOX/- MEFs. The experiment was performed in duplicate and expression levels are shown as mean ± standard deviation. **(b)** qRT-PCR performed as above but showing no significant changes in *Gli2* mRNA expression in Cre-treated Snf5FLOX/- MEFs.

Nature Medicine: doi:10.1038/nm.2251

a

Gli1

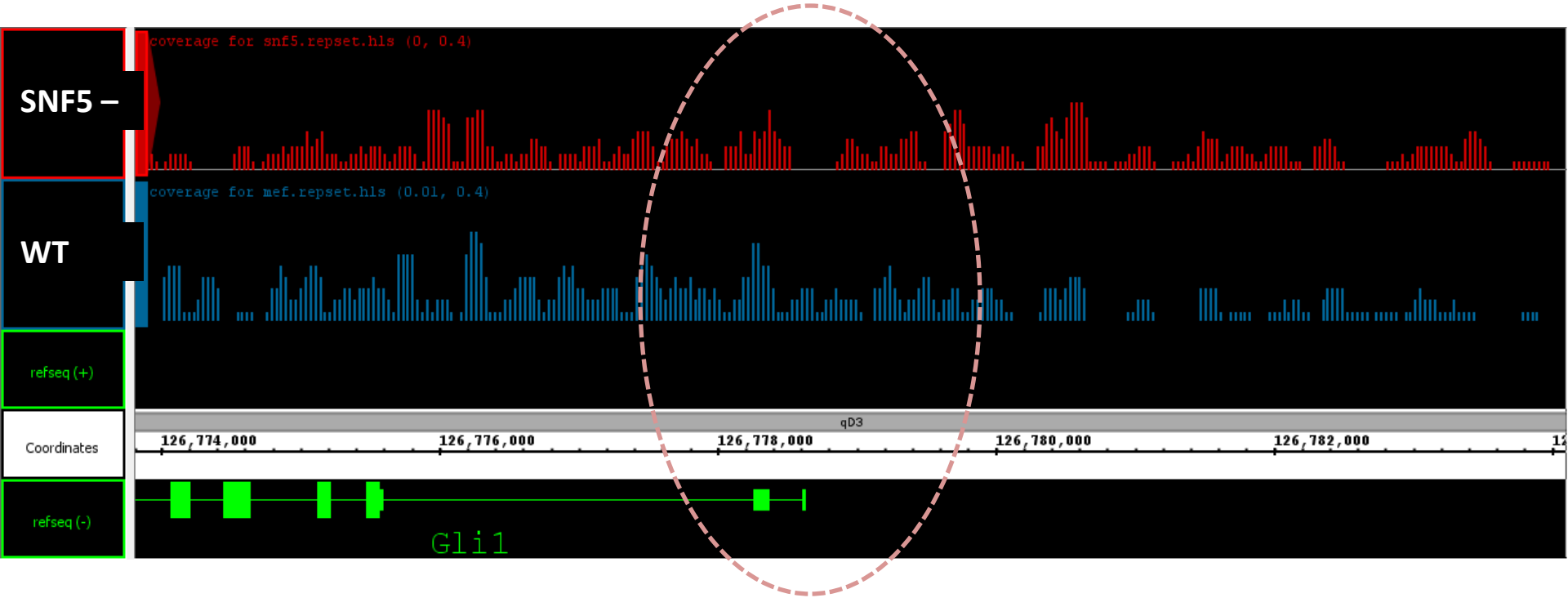

direction of transcription

Ratio of normalized numbers of tags within 1.5 kb of TSS in SNF5 and WT samples is 0.7 ($P<0.05$)

Nature Medicine: doi:10.1038/nm.2251

b

Ptch1

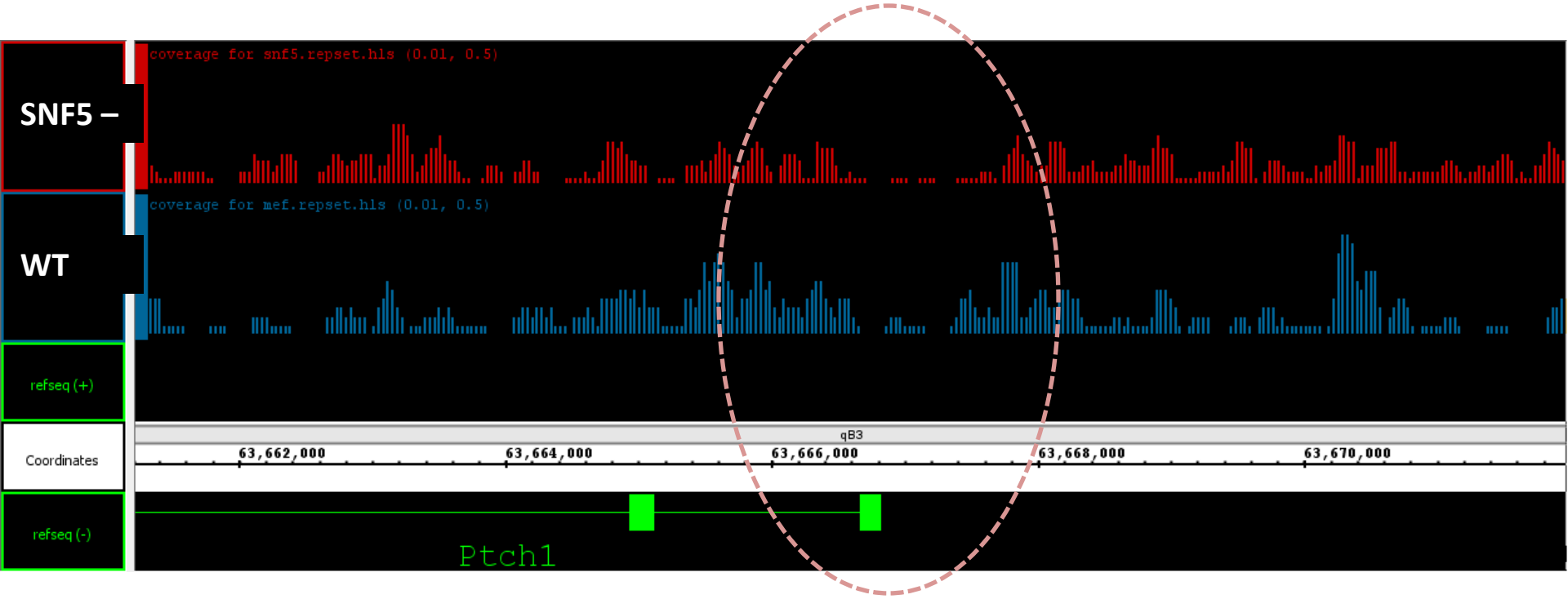

direction of transcription

Ratio of normalized numbers of tags within 1.5 kb of TSS in SNF5 and WT samples is 0.5 (P<0.001)

Nature Medicine: doi:10.1038/nm.2251

Supplementary Figure 4. **Nucleosome occupancy around transcription starts of *Gli1* (a) and *Ptch1* (b) genes.** The nucleosome occupancy profiles as measured by sequencing of MNase-digested mononucleosomal fragments for Snf5 deficient (red) and wild type (blue) cells are shown in each figure. The dashed white lines mark regions ±1 kb around the transcription start of each gene. The counts of nucleosome fragments with the centers located within these regions are significantly lower in Snf5-deficient cells as compared to the corresponding counts in wild type cells ($P<0.05$ for Gli1 gene and $P<0.001$ for Ptch1 gene, Fisher's test).

Nature Medicine: doi:10.1038/nm.2251

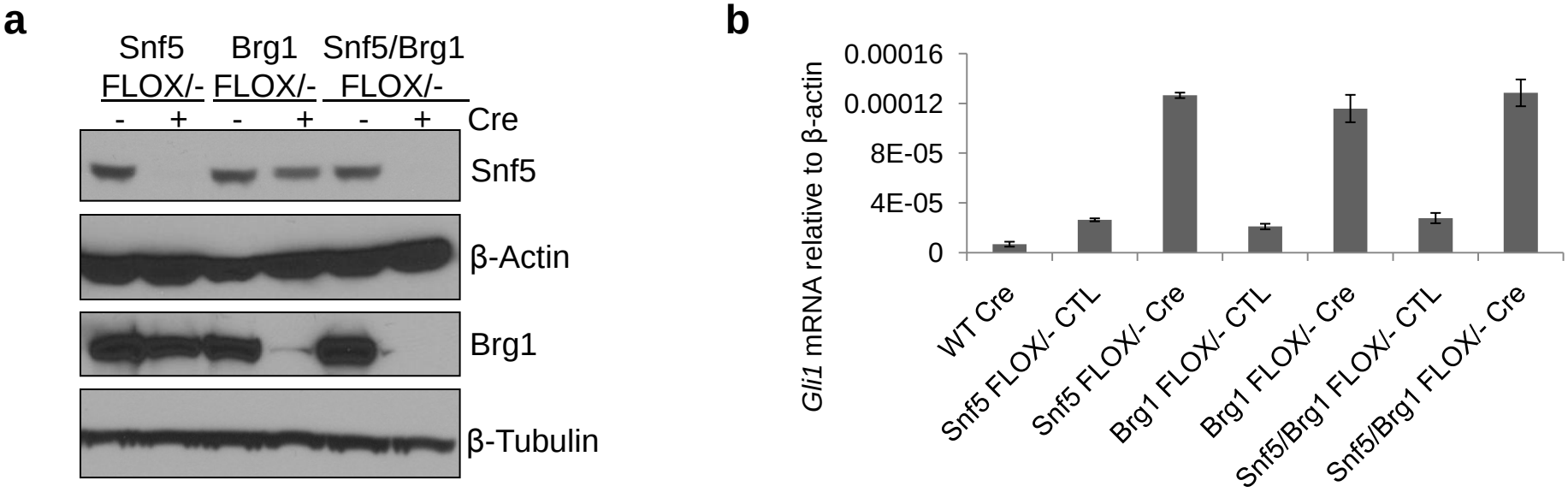

Supplementary Figure 5 . The core Swi/Snf5 subunit Brg1 is also essential for the repression of Gli1 expression. (a) Immunoblot showing loss of Snf5, Brg1, or both Snf5 and Brg1 protein in Cre recombinase treated Snf5FLOX/- , Brg1 FLOX/- or Snf5/Brg1FLOX/- primary mouse embryonic fibroblasts (MEFs) respectively. (b) QRT-PCR showing up-regulation of *Gli1* mRNA in Cre-treated Snf5FLOX/- , Brg1 FLOX/- or Snf5/Brg1FLOX/- primary MEFs. The experiment was performed in duplicate, and expression levels are shown as mean ± standard deviation.

Nature Medicine: doi:10.1038/nm.2251

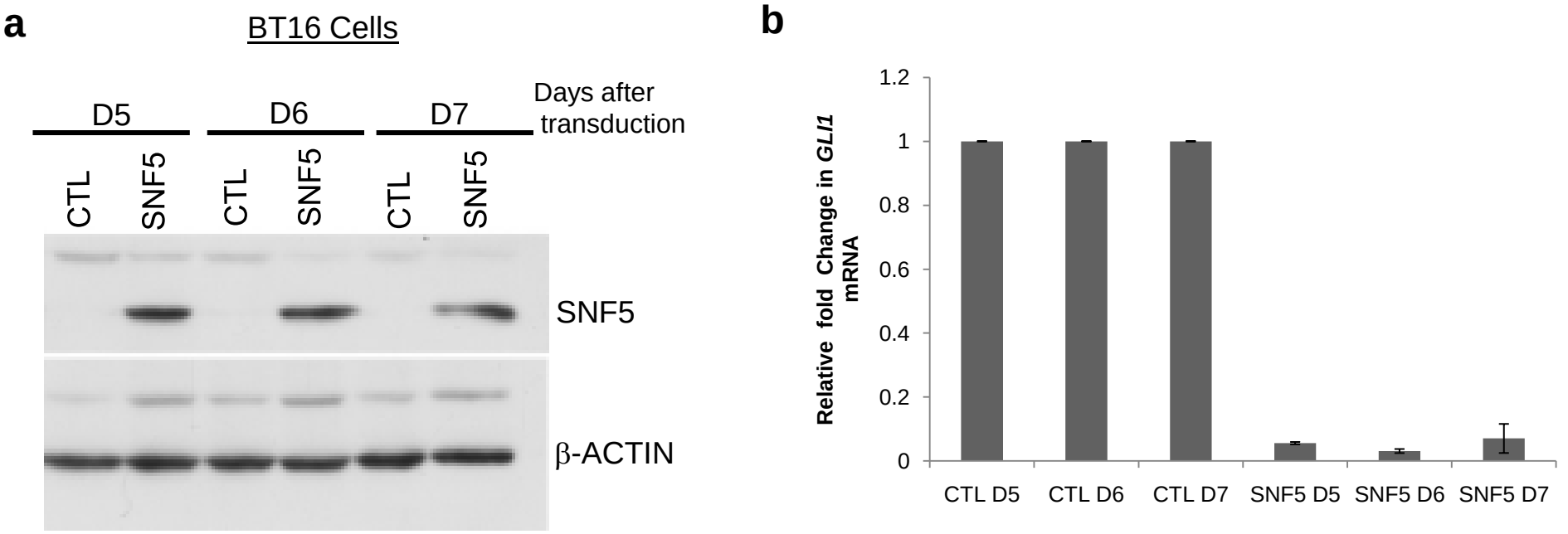

Supplementary Figure 6. Re-introduction of SNF5 represses GLI1 expression in SNF5-deficient BT16 cells. (a) Immunoblot showing expression of SNF5 in BT16 cells after 5, 6, and 7 days (D5, D6, D7) of retroviral infection with a SNF5 expressing vector but not control vector (CTL). **(b)** QRT-PCR showing reduction in GLI1 expression in SNF5-expressing BT16 cells. The experiment shown is representative of three independent experiments and values represent mean ± standard deviation of triplicate samples.

Nature Medicine: doi:10.1038/nm.2251

a

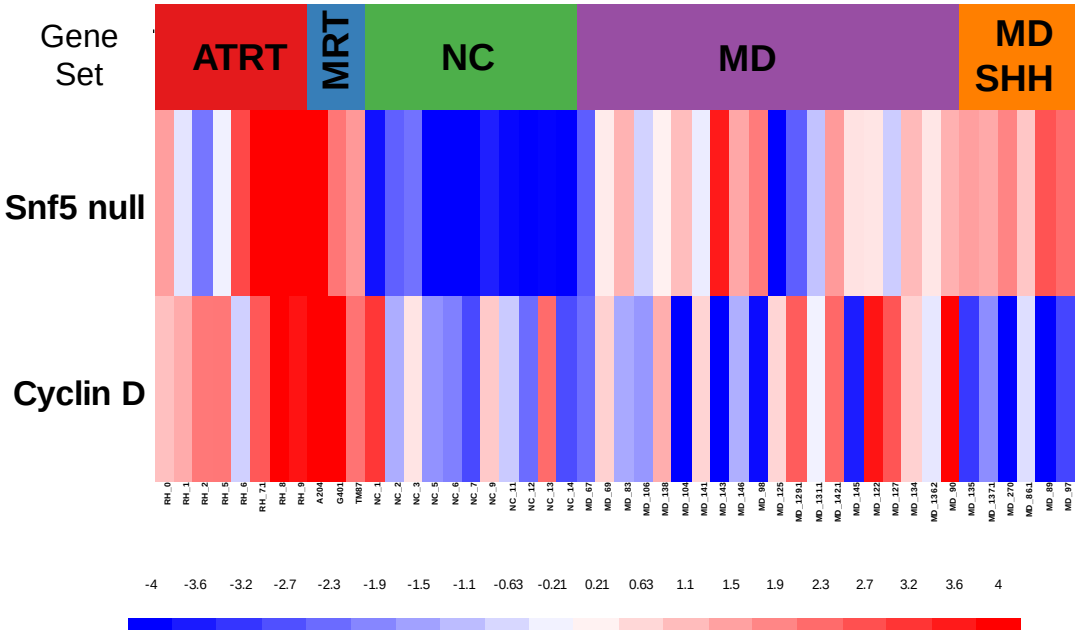

b

Snf5 null/Up, GLI1-Up Regulated Genes	Snf5 null/Down, GLI1-down Regulated Genes
OASL1	HOXA5
PSMB8	SYTL2
VAMP5	SLCO3A1
CXCL10	MGST2
OLIG1	ANKRD1
ENPP3	NSG1
TAP2	SIM2
AURKB	DSCR1L1
PSMB9	
TAPBP	
CXCR4	

Supplementary Figure 7. Snf5 null and CyclinD expression signatures in primary rhabdoid tumors. **(a)** Heatmap showing the single-sample signature profiles of signatures for Snf5 null and Cyclin D in a multi-tumor gene expression panel. ATRT (primary brain rhabdoid tumors), MRT cell (3 MRT cell lines), NC (Normal cerebellum), MD (medulloblastoma), MD Shh (Medulloblastoma samples with activation of the Hh pathway). For the ATRT samples, p= .015 for the Snf5 null gene set, and p= 0.00669 for the Cylin D gene set. The signature descriptions and signature projection methodology are described in methods. **(b)** List of GLI1 induced up-regulated and down regulated genes that overlap with the Snf5 null up-regulated (7% overlap, 11/150 genes) and down-regulated (6% overlap, 8/138 genes) respectively.

Nature Medicine: doi:10.1038/nm.2251

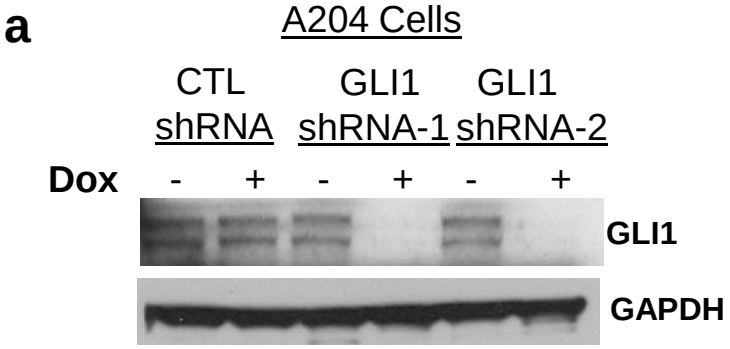

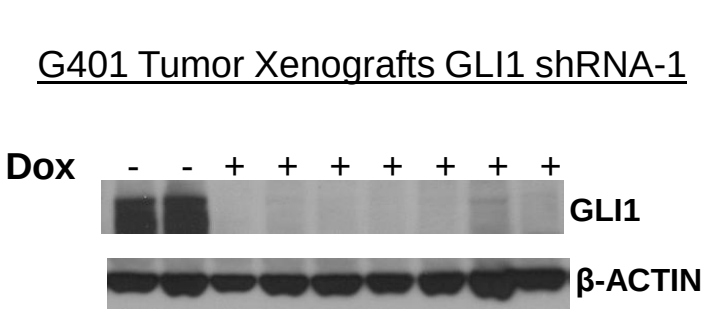

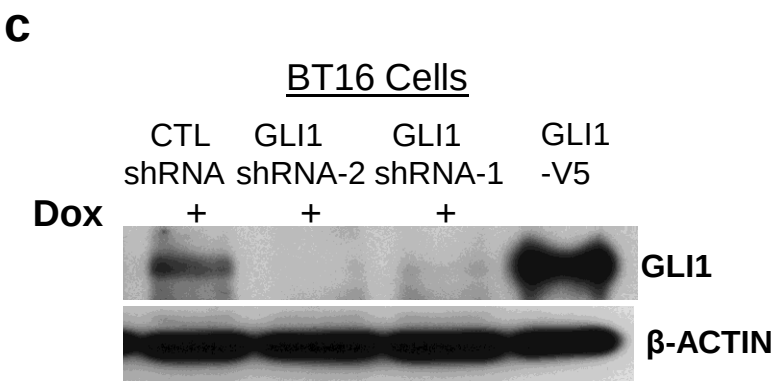

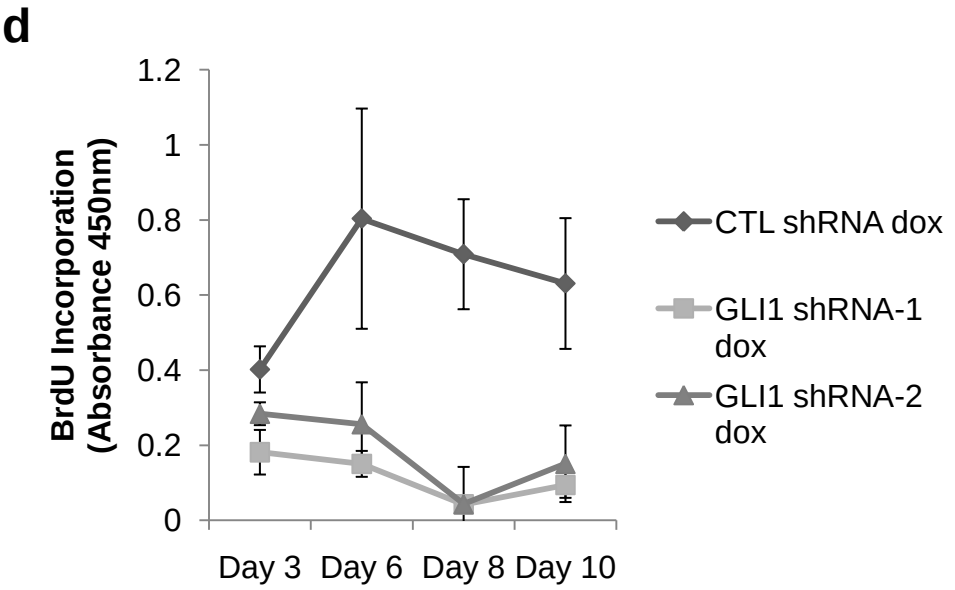

Supplementary Figure 8. GLI1 depletion inhibits proliferation of additional MRT cell lines. (a) Immunoblot showing reduction of endogenous GLI1 protein in A204 cells upon induction of two independent GLI1 shRNAs with Doxycycline (72 hrs, 100ng/mL). GAPDH shows equal loading. **(b)** Immunoblot showing depletion of GLI1 in dox treated G401 GLI1shRNA tumors. **(c)** Immunoblot showing reduction of GLI1 protein in BT16 cells upon Dox induction of GLI1 shRNAs but not CTL shRNAs. **(d)** BT16 cells were treated with Dox for 3 days, and seeded for the BrdU assay on Day 3. Dox treatment was continued through the time course and Dox induction of GLI1 shRNAs but not CTL shRNAs led to decreased BrdU incorporation.

Nature Medicine: doi:10.1038/nm.2251

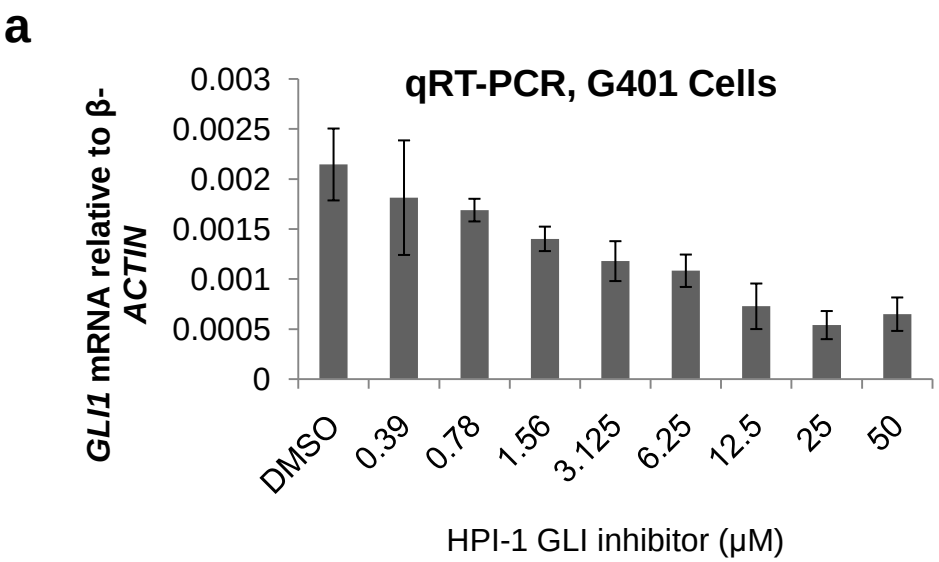

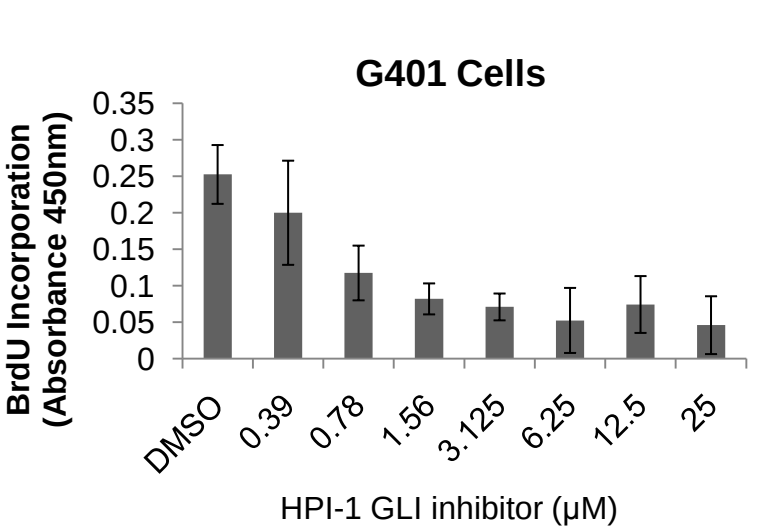

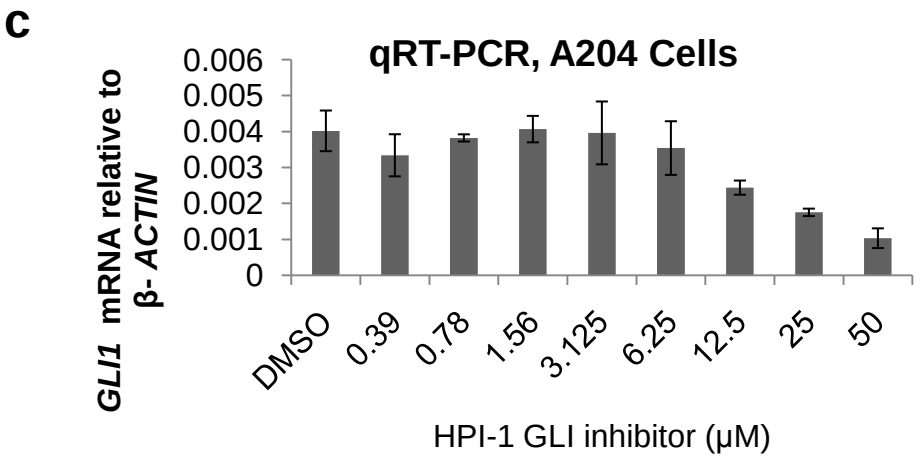

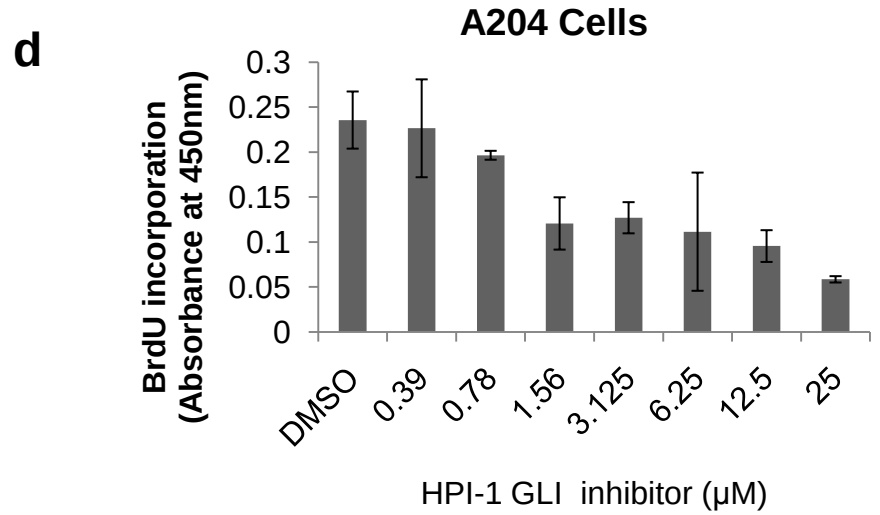

Nature Medicine: doi:10.1038/nm.2251

Supplementary Figure 9. Pharmacologic Inhibition of GLI1 inhibits proliferation of MRT cells. (a) QRT-PCR demonstrating dose-dependent decreases in GLI1 mRNA measured after 24 hours treatment of G401 cells with HPI-1. The concentrations at which these effects were observed are well within the range reported to inhibit GLI1 over-expression induced activation of the Gli-luciferase reporter (IC50 of 6 μM) or inhibit GLI1 expression in constitutively active Smo-M2 dependent cerebellar granule neuron precursors (20 μM) (Ref 25, Hyman et al., 2009). Each experiment was performed in triplicate and is a representative of at least three independent experiments. (b) BrdU assays showing the corresponding decrease in cell proliferation (G401 cells) measured 3 days after treatment. (c) Performed as in A above, but for A204 cells. (d) Performed as in B above, but for A204 cells and measured after 6 days of HPI-1 treatment. All values shown represent mean ±standard deviation.

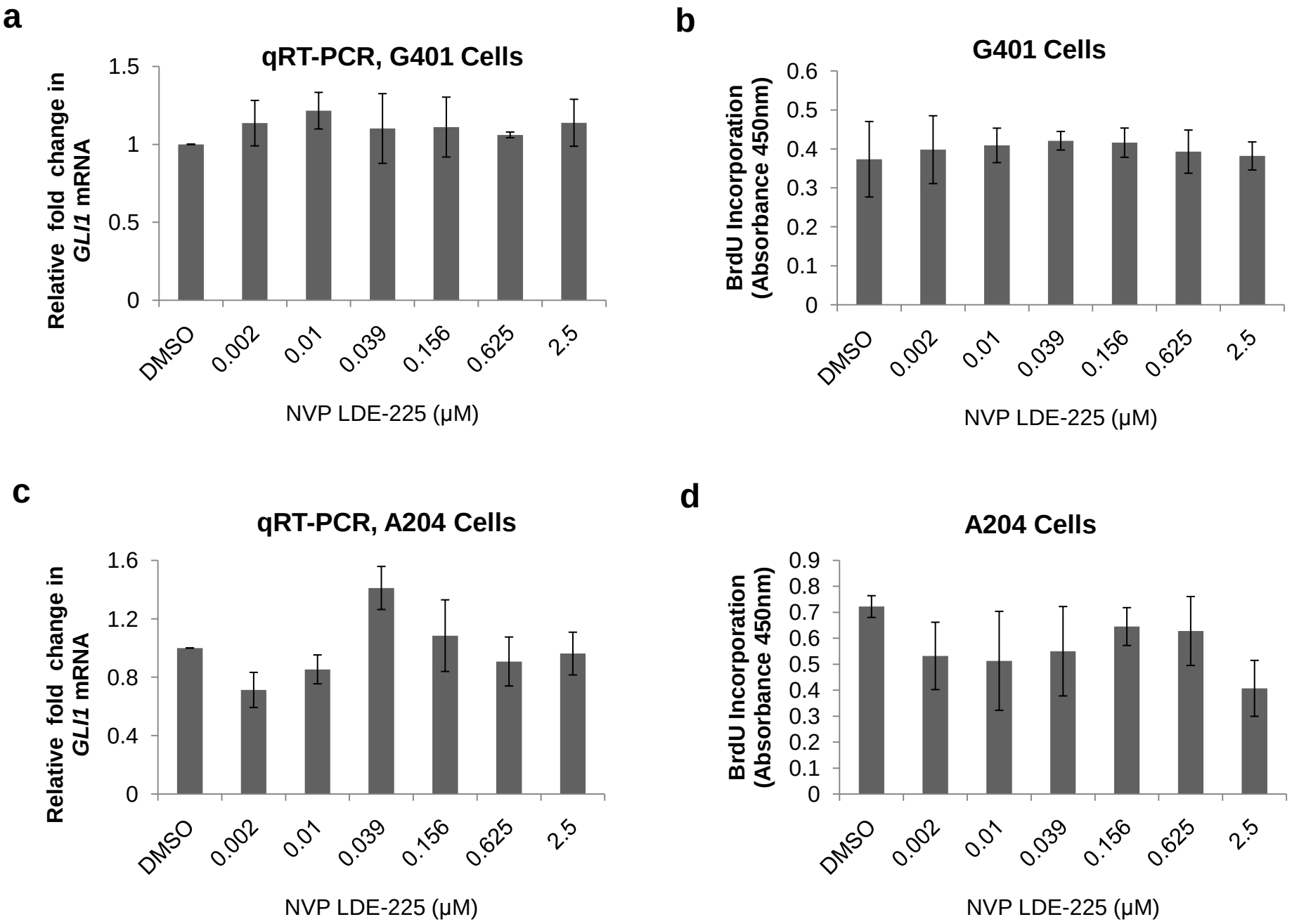

Nature Medicine: doi:10.1038/nm.2251

Supplementary Figure 10. Pharmacologic Inhibition of SMO does not affect GLI1 expression nor proliferation of MRT cells. (a) QRT-PCR demonstrating similar levels of GLI1 mRNA as measured after 24 hours treatment of G401 cells with a highly specific SMO antagonist NVP LDE-225. The highest concentration used in this experiment (in the micromolar range) is well above the IC50 (0.6nM) reported for this compound in the Agonist 1.5 (1nM) induced Gli-Luciferase reporter assay. **(b)** BrdU assays after 3 days of treatment with NVP LDE-225 showing no changes in cell proliferation (G401 cells). **(c)** Performed as in a above, but for A204 cells. **(d)** Performed as in b above, but for A204 cells. All values shown represent mean ±standard deviation.

Nature Medicine: doi:10.1038/nm.2251

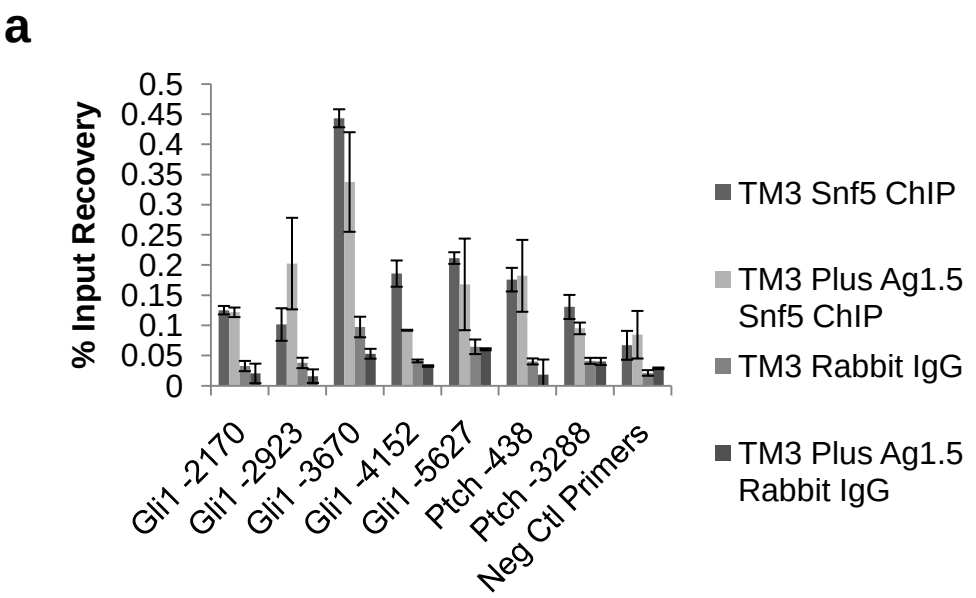

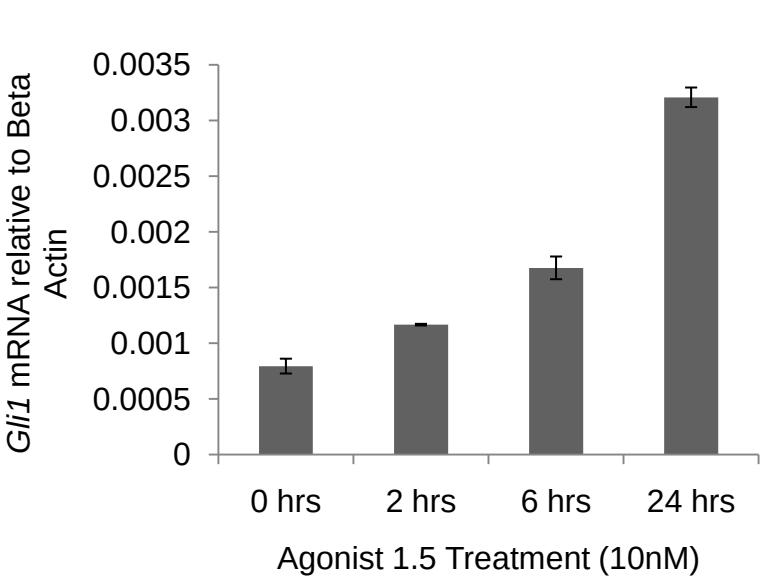

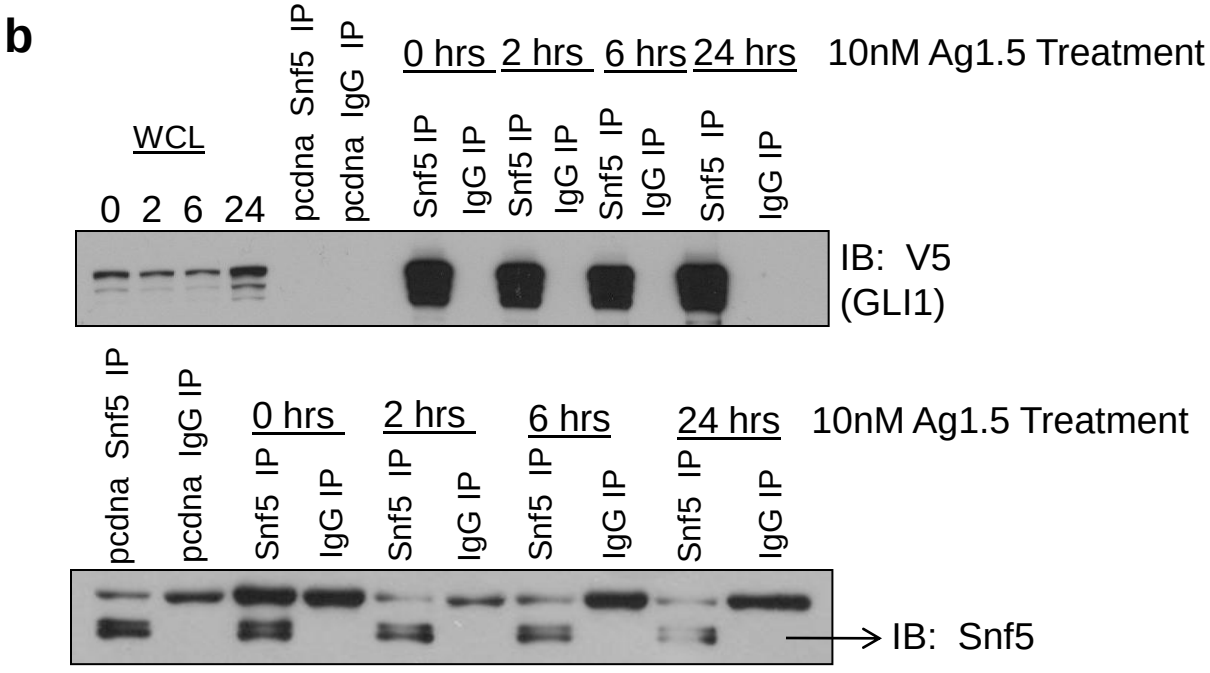

Nature Medicine: doi:10.1038/nm.2251

Supplementary Figure 11. Stimulation of the Hh pathway with Agonist 1.5 does not alter Snf5 localization to Gli1 regulated promoters nor its interaction with GLI1. **(a)** Chromatin Immunoprecipitation (ChIP) assay showing enrichment of Snf5 at *Gli1* and *Patched1* promoters in the absence and presence of Hh pathway stimulation with Agonist 1.5. (24 hrs, 25nM) **(b)** Whole cell lysates from TM3 cells over-expressing V5 taqgged WT GLI1 were treated in a time course of Agonist 1.5 (10nM for 0, 2, 6, 24hrs) and subjected to immunoprecipitation (IP) of endogenous Snf5 with a Snf5 antibody or a control IgG. Subsequent immunoblotting (IB) with a V5 antibody revealed co-immunoprecipitation of WT GLI1 under all conditions. A control blot indicating immunoprecipitation of Snf5 is shown below. **(c)** A control qRT-PCR confirming the expected increase in *Gli1* transcripts upon stimulation of the Hh pathway with Agonist 1.5 treatment. Experiment was performed in triplicate and expression levels are shown as mean ± standard deviation.

Supplementary Methods

Cell Culture

TM3, A204, and G401 cells were obtained from ATCC and BT16 from Dr. David James (UCSF). Cells were cultured in DMEM, 10% FBS, 1% L-Glutamine, and 50 M -Mercaptoethanol. TM3 cells were cultured in F-12/D-MEM (1:1), 1% L-Glutamine, 5% Horse Serum, 2.5% FBS and 15 mM HEPES

TAP-Tagged Proteins/Mass Spectrometry/Statistical Methods

Human GLI1 was tagged at the C-terminus using the TAP tag (C-TAP) and stably expressed in TM3 cells by retrovirus-mediated gene transfer [1]. GLI1 transduction was verified by immunoblot and GLI1-TAP-containing protein complexes were subsequently purified from nuclear extracts and subjected to 1D SDS-PAGE. Gel lanes were cut into slices across the full separation range and subjected to in-gel tryptic digestion. Peptide mass and fragmentation data obtained by liquid chromatography-tandem mass spectrometry were used to query an in-house curated version of the IPI database using Mascot (Matrix Science) [1]. The statistical significance of the interactions between tagged GLI1 and the detected Smarc proteins was calculated using binomial statistics. To this end, the frequency with which the Smarc proteins bound distinct tagged proteins in our internal database was determined, controlling for the number of detected peptides, the lysis conditions used, and the cell line species of origin. Using these background frequencies, the binomial probability of each Smarc protein detection across the GLI1 protein complex immunopurifications in mouse cells was calculated and corrected for multiple hypothesis tested to arrive at the final Expected (E) values (the product of the p-values and the number of tested hypotheses) as well as False Discovery Rate-corrected p-values. Similarly, we

calculated the significance of all detected proteins' association with tagged GLI1 using E values and the strength of their association with tagged GLI1 using $\log_{10}$ fold ratios of those detected protein frequencies in the GLI1 pulldowns relative to their background frequencies in mouse cells: these statistics together were used to confirm the selectivity of tagged GLI1's interactions, particularly with the Smarc proteins.

Transient Transfection/Co-immunoprecipitation/Immunoblots

TM3 cells or G401 cells were transiently transfected with either vector control (pcdna3.1) or Gli1-V5-pcdna3.1 constructs using Lipofectamine 2000 (Invitrogen) and Fugene HD reagent (Roche) respectively. Cells were harvested after 48 hours in lysis buffer containing 50 mM Tris pH 7.4, 1.5 mM MgCl2, 100 mM NaCl, 25 mM NaF, 1 mM Na3VO4, 0.2% NP-40, 1 mM DTT and a complete protease inhibitor tablet (Roche). Lysates were cleared by centrifugation and directly used for immunoprecipitation. Primary antibodies used were either monoclonal Snf5 (Smarcb1) (BD Biosciences) or mouse IgG antibodies (Santa Cruz Biotech). Antibodies used for immunoblot detection include anti-V5 antibody (Invitrogen), anti-GLI1 antibody (V812) (Cell Signaling Tech.) and anti-Snf5 antibody (Bethyl laboratories).

Q-PCR for Chromatin Immunoprecipitation (ChIP) assay

Q-PCR was performed using the power SYBR green master mix (Applied Biosystems) with the following primer sets (5'-3'): Gli1 mouse promoter primers: -966 F GTTCCGTTCCCCATTTTACC, -966 R TCCACTCCAGGTTTTTCAGC, -2110 F CCCGCTCTGAATCCTCTTTC, -2110R CCTTTCCTTGATGCTGTTCC, -2923 F TATGGGGTTGGGAGAGTTTG, -2923 R AAAGAGACCTGGGACAGACAC, -3670 F ATGGGGAAAGCTCAGTTACG, -3670 R TGAACCAGAGCCAGGAAAAC, -5627 F CACTGGGAAGACAGAAGCAAG, -5627 R GCCCCTGATTGGATGATTG, Ptch -438 F

TGG GTG GTC TCT CTA CTT TGG, Ptch-438 R TGT CAG ATG GCT TGG GTT TC, Ptch-3288 F ACT GGC TCC TCT TCC CTT TC, and Ptch-3288 R GCT TCC CCT GTG GTC TGC. Mouse IGX1A Negative Control Primers (SABiosciences cat # GPM00001C(-)01A).

shRNA and Expression Constructs

Sequences used for shRNA mediated knock down of Snf5 were from the RNAiCodex database [2]. Snf5 –TGC TGT TGA CAG TGA GCG CGC TAA TGA CTC CTG AGA TGT TTA GTG AAG CCA CAG ATG TAA ACA TCT CAG GAG TCA TTA GCT TGC CTA CTG CCT CGGA Scrambled control shRNA-TGC TGT TGA CAG TGA GCG CGA TCC AAC TTA TGT GGC AGT TTA GTG AAG CCA CAG ATG TAA ACT GCC ACA TAA GTT GGA TCT TGC CTA CTG CCT CGGA. Oligos matching these sequences were synthesized, PCR amplified using the following primers, GAT GGC TGC TCG AG AAG GTA TAT TGC TGT TGA CAG TGA GCG and GTC TAG AGG AAT TCC GAG GCA GTA GGCA, digested with the restriction enzymes Xho1 and EcoR1, and subsequently cloned into a microRNA adapted retroviral vector (MSCV-LTRmiR30-PIG, Open Biosystems). Retrovirus was made using the packaging vector pCLECO[3] in 293T cells. The GLI1 shRNAs (3414-GLI1 shRNA-2) CATCCATCACAGATCGCATTT and (2761-GLI1 shRNA-1) GCTCAGCTTGTGTGTAATTAT were cloned into the dox inducible pLKO-Tet-On lentiviral vector (puromcyin) and packaged into lentivirus as previously described [4].

Retroviral Infection of TM3 Cells

500,000 TM3 cells were seeded on 10cm 0.1% gelatin coated dishes and infected the next day with 1mL of retroviral supernatant in a final concentration of 8 g/mL of polybrene (Chemicon) (4mL total volume). After 4 hours at 37 C, medium was

removed, and cells were re-infected as above. After another 4 hours, medium was replaced. 48 hours post-infection, cells were sorted for the top 20% GFP expressing cells, and were subsequently treated with puromycin. 48 hours after sorting, cells were harvested for downstream Q-RT-PCR and Western blot analyses.

SNF5 Re-Expression

SNF5-deficient G401 cells were transduced using either pBabe-puro^r-FLAG-SNF5 (generously provided by Robert E. Kingston, Massachusetts General Hospital) or pBabe-puro^r-Empty two times at 4 hour intervals followed by selection in puromycin (1 g/ml) for 48 h then harvested at 48 hours and later time points for RNA or protein analysis

Lentiviral Infection of Malignant Rhabdoid Tumor (MRT) Cell Lines

Lentiviral infection of MRT cells was performed by plating 150,000 cells in a 6 well plate, and infecting the next day with 1mL of lentiviral supernatant in the presence of polybrene (10 g/mL). Cells were spinfected for 1hour (800G) at room temperature. Medium was replaced the following day and stable pools of cells were selected with 1-2 g/mL of puromycin.

Quantitative RT-PCR (qRT-PCR)

mRNA levels were measured using the ABI PRISM 7900 HT Sequence Detection System (Applied Biosystems, ABI). ABI taqman gene expression assays include: Human: Gli1 (Hs00171790_m1), Gli2 (Hs00257977_m1), Ptch1 (Hs00181117_m1), Smarcb1 (Hs_00268260_m1), Smo(Hs01090242) Mouse: Gli1 (Mm00494645_m1), Gli2 (Mm01293110_m1), Smo (Mm01162710_m1), Ptch1(Mm 00436026_m1), Smarcb1 (00448776_m1). VIC-MGB -actin primers/probe (Applied Biosystems) were used in each reaction to co-amplify the -actin transcript. All experiments were performed in either duplicate or triplicate and normalized to -actin levels. Relative

mRNA expression is given by the formula $2^{-(C_T \text{ of sample} - C_T \text{ of ß-actin})}$, where C_T (cycle count) is the threshold cycle value.

Signature (Gene Sets) Description

Hh signaling pathway: Gene set HSA04340_HEDGEHOG_SIGNALING_PATHWAY from the MSigDB -C2 database (http://www.broad.mit.edu/gsea/msigdb) , containing 57 genes involved in Hedgehog signaling pathway (Original KEGG pathway HSA04340).

Basal Cell Carcinoma: Gene set HSA05217_BASAL_CELL_CARCINOMA from the MSigDB -C2 database (http://www.broad.mit.edu/gsea/msigdb) , containing 56 genes involved in in basal cell carcinoma (Original KEGG pathway HSA05217).

Snf5 null: Signature combining the top 200 (200) up-(down-) regulated genes (selected by difference of means) identified by Snf5 knockout as described in [5].

Cyclin D: Signature combining the top 200 (200) up-(down-) regulated genes (selected by difference of means) identified by Cyclin D over-expression as described in [6].

GLI1: Signature combining the top 30 (30) up-(down-) regulated genes (selected by difference of means) identified by GLI1 stable expression as described in [7]. In this case the size is 30 rather than 200 like in the other signatures because this signature was refined as a predictor of desmoplastic vs. classic medulloblastoma histology on a separate dataset. The actual gene sets definitions can be provided in a gene_sets.xls file upon request.

Growth Assays

HPI-1 inhibitor (Ryan Scientific) was dissolved at 10 mM in DMSO. A204 and G401 cells were seeded at 2500 and 5000 cells/well respectively in 0.5% serum medium. Cells were treated the following day (maintaining a constant 0.5% DMSO

concentration across all compound concentrations), and cell proliferation was measured after 72 hours or 6 days using the cell proliferation ELISA, BrdU (colorimetric) (Roche Applied Science) kit. Cell proliferation assays upon shRNA mediated knockdown of GLI1 were performed by seeding 1000 cells per well in a 96 well (triplicate) and treatment in the absence and presence of Dox. BrdU measurements were taken at several time points to track cell proliferation and were calculated as percentage of cells with BrdU incorporation over untreated controls. Focus formation assays were carried out by inducing GLI1 and Control (CTL) non-targeting shRNAs with Doxycycline (100ng/mL) for 3 days, followed by seeding 500-2000 cells/well of a 6 well plate in triplicate, and continuing treatment with dox every 2-3 days. After 14 days, colonies were visualized by staining with Crystal violet.

Nucleosome Repositioning Assays

Wild-type or Snf5-deficient cells were harvested, washed in PBS, and re-suspended in 2 mL low detergent buffer [0.3M Sucrose, 15mM Tris-Cl (pH 7.6), 60mM KCl, 15mM NaCl, 5mM $MgCl_2$, 0.1mM EDTA, 0.5mM DTT, 0.4% NP-40] for 10 minutes to lyse cells. The cell solution was layered on 8 mL high sucrose buffer [1.2M sucrose, 60mM, KCl, 15mM NaCl, 5mM $MgCl_2$, 0.1mM EDTA, 0.5mM DTT] and spun at 10,000xg to pellet nuclei. Isolated nuclei were resuspended in 1 mL micrococcal nuclease (MNase) buffer [0.32 sucrose, 50mM Tris-Cl (pH 7.6), 4mM $MgCl_2$, 1mM $CaCl_2$]. MNase digestion, was carried out using 30 units of enzyme to yield approximately 6% mono-nucleosomes. DNA fragments (150 bp) were RNAse treated, precipitated, gel-extracted and prepared for Helicos sequencing. DNA fragments were subjected to massively parallel sequencing on a HeliScope Single Molecule Sequencer, and then mapped to the mouse genome (mm9) using Bowtie aligner [8]. Nucleosome occupancy was computed by extending each sequenced tag by 150 bp towards its 3'-end and

counting the number of overlapping fragments at each genomic coordinate. The tag counts were normalized to one million of sequenced tags in each sample. Coordinates of transcription start sites were taken from the USCS track RefGene for mouse genome [9]. Integrated Genome Browser was used for nucleosome occupancy visualization [10].

Supplementary Methods References

1. Bouwmeester, T. et al. A physical and functional map of the human TNF-alpha/NF-kappa B signal transduction pathway. *Nat Cell Biol* **6**, 97-105 (2004).
2. Olson, A., Sheth, N., Lee, J.S., Hannon, G. & Sachidanandam, R. RNAi Codex: a portal/database for short-hairpin RNA (shRNA) gene-silencing constructs. *Nucleic Acids Res* **34**, D153-7 (2006).
3. Naviaux, R.K., Costanzi, E., Haas, M. & Verma, I.M. The pCL vector system: rapid production of helper-free, high-titer, recombinant retroviruses. *J Virol* **70**, 5701-5 (1996).
4. Wiederschain, D. et al. Single-vector inducible lentiviral RNAi system for oncology target validation. *Cell Cycle* **8**, 498-504 (2009).
5. Isakoff, M.S. et al. Inactivation of the Snf5 tumor suppressor stimulates cell cycle progression and cooperates with p53 loss in oncogenic transformation. *Proc Natl Acad Sci U S A* **102**, 17745-50 (2005).
6. Lamb, J. et al. A mechanism of cyclin D1 action encoded in the patterns of gene expression in human cancer. *Cell* **114**, 323-34 (2003).
7. Yoon, J.W. et al. Gene expression profiling leads to identification of GLI1-binding elements in target genes and a role for multiple downstream pathways in GLI1-induced cell transformation. *J Biol Chem* **277**, 5548-55 (2002).
8. Langmead, B., Trapnell, C., Pop, M. & Salzberg, S.L. Ultrafast and memory-efficient alignment of short DNA sequences to the human genome. *Genome Biol* **10**, R25 (2009).
9. Kuhn, R.M. et al. The UCSC Genome Browser Database: update 2009. *Nucleic Acids Res* **37**, D755-61 (2009).
10. Nicol, J.W., Helt, G.A., Blanchard, S.G., Jr., Raja, A. & Loraine, A.E. The Integrated Genome Browser: free software for distribution and exploration of genome-scale datasets. *Bioinformatics* **25**, 2730-1 (2009).